Accepted Manuscript

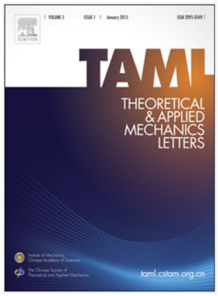

Amodified airfoil-based piezoaeroelastic energy harvester with double plunge degrees of freedom

Yining Wu, Daochun Li, Jinwu Xiang, Andrea Da Ronch

PII: S2095-0349(16)30047-2
DOI: http://dx.doi.org/10.1016/j.taml.2016.08.009
Reference: TAML 101

To appear in: *Theoretical and Applied Mechanics Letters*

Received date: 7 June 2016
Revised date: 3 July 2016
Accepted date: 7 August 2016

Please cite this article as: Y. Wu, D. Li, J. Xiang, A. Da Ronch, Amodified airfoil-based piezoaeroelastic energy harvester with double plunge degrees of freedom, *Theoretical and Applied Mechanics Letters* (2016), http://dx.doi.org/10.1016/j.taml.2016.08.009

Amodified airfoil-based piezoaeroelastic energy harvester with double plunge degrees of freedom

Yining Wu[a], Daochun Li[a], Jinwu Xiang[a*], Andrea Da Ronch[b]

[a]*School of Aeronautic Science and Engineering, Beihang University, Beijing 100191, China*

[b]*Engineering and the Environment, University of Southampton, Southampton SO171BJ, UK*

Abstract

In this letter, a piezoaeroelastic energy harvester based on an airfoil with double plunge degrees of freedom is proposed to additionally take advantage of the vibrational energy of the airfoil pitch motion. An analytical model of the proposed energy harvesting system is built and compared with an equivalent model using the well-explored pitch-plunge configuration. The dynamic response and average power output of the harvester are numerically studied as the flow velocity exceeds the cut-in speed (flutter speed). It is found that the harvester with double-plunge configuration generates 4% to 10% more power with varying flow velocities while reducing 6% of the cut-in speed than its counterpart.

Keywords

energy harvesting; aeroelastic; airfoil; piezoelectric

[*]Correspondingauthor. E-mail address: xiangjw@buaa.edu.cn (J. Xiang).

Introduction

The objective of energy harvesting (EH) is to convert ambient energy such as solar, tidal, and wind energy into available electric energy. Recently, EH based on aeroelastic vibrations has received growing attention since it potentially out performs the conventional turbines in terms of small scale wind EH [1].The harvested energy can be used for low-power electronic systems such as wireless sensor networks to reduce cabling and maintenance costs [2].

Taking advantage of aeroelastic phenomena, several harvesters have been designed, manufactured, and tested based on flutter of cantilevered plates [3,4],galloping oscillations of bluff bodies [5,6],wake galloping phenomenon [7,8], and vortex-induced vibrations [9,10]. Airfoil-based energy harvesters, exploiting aeroelastic vibrations, consist of a rigid airfoil with supporting devices that allow the pitch-plunge vibrations of the airfoil with transducers coupled to the plunge degree of freedom (DOF) [11,12].Towards airfoil-based harvesters, a large body of work has been done including analytical modeling and experimental activities [13,14], investigating the effects of structural nonlinearities [15-18] and system parameters [19-23] to improve EH performance, and analyzing EH under the combined base and wind excitations [24,25]. Cambered airfoils [26] and 3-DOF airfoils with control surfaces [27-28] were also considered to enhance design flexibility.

Previous studies on piezoaeroelastic EH of airfoil-based harvesters used a pitch-plunge configuration with piezoelectric transducers coupled to the plunge DOF. The airfoils were generally held by torsional springs and rotating shafts connected to cantilevered piezoelectric beams. The coupling between the transducers and the pitch DOF was not considered in the previous studies because (a) it is difficult to attach the piezoelectric transducers to the torsional springs, and (b) it is relatively hard to convert the airfoil pitch motion into the deformation of the piezoelectric materials compared with the use of the piezoelectric beams. From an EH point of view, however, the vibrational energy in the pitch DOF was not converted into electric energy and wasted. The objective of this letter is to enhance the performance of airfoil-based harvesters by additionally taking advantage of the vibrational energy of the airfoil pitch motion.

Modified Design and Analytical Model

As it is very difficult to couple the piezoelectric transducers to the pitch DOF, an airfoil with double plunge supporting devices is used. Shown in Fig. 1, a second plunge DOF is introduced instead of the pitch DOF. The mechanical energy of each plunge DOF is converted into electric energy via the corresponding transducer and then consumed by a load resistance in the respective circuit.

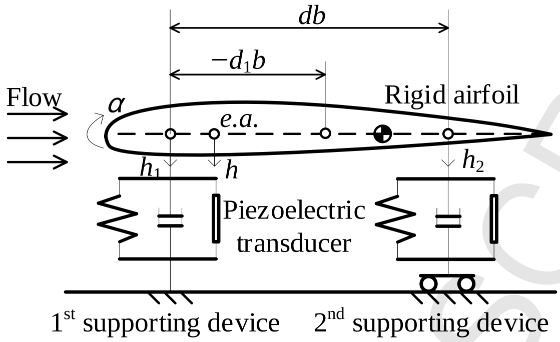

Fig. 1. Schematic of the airfoil-based harvester with double plunge DOFs.

Shown in Fig. 1, the displacements of two plunge supporting devices are denoted by h_1 and h_2, positive downward. The terms d_1 and a denote, respectively, the dimensionless offset of the first supporting device and the elastic axis from the airfoil mid-chord. The term d is the dimensionless offset of the second supporting device measured from the first one. The location of the elastic axis is determined by $a=d_1+k_2d/(k_1+k_2)$, where k_1 and k_2 are the linear stiffness coefficients of the two plunge DOFs, respectively, including the contributions from both the plunge springs and transducers. The dynamic equations of the proposed double-plunge airfoil-based piezoaeroelastic harvester are derived as

$$\begin{aligned}&\left[m\left(\frac{d-d_c}{d}\right)^2+\frac{J_c}{db^2}+m_1\right]\ddot{h}_1+\left[\frac{md_c(d-d_c)}{d^2}-\frac{J_c}{db^2}\right]\ddot{h}_2+c_1\dot{h}_1+k_1h_1-\theta V_1\\&=-\frac{(1+a+4d+4d_1)}{4d}\left[L\cos(\alpha_{\text{eff}}-\alpha)+D\sin(\alpha_{\text{eff}}-\alpha)\right]-\frac{M}{db},\end{aligned} \tag{1}$$

$$\begin{aligned}&\left[\frac{md_c(d-d_c)}{d^2}-\frac{J_c}{db^2}\right]\ddot{h}_1+\left[m\left(\frac{d_c}{d}\right)^2+\frac{J_c}{db^2}+m_2\right]\ddot{h}_2+c_2\dot{h}_2+k_2h_2-\theta V_2\\&=-\frac{(1-2a+4d_1)}{4d}\left[L\cos(\alpha_{\text{eff}}-\alpha)+D\sin(\alpha_{\text{eff}}-\alpha)\right]+\frac{M}{db},\end{aligned} \tag{2}$$

$$V_1/R_1+\theta\dot{h}_1+C_p\dot{V}_1=0,\ V_2/R_2+\theta\dot{h}_2+C_p\dot{V}_2=0, \tag{3}$$

where $d_c=a-d_1+x_\alpha$, and x_α is the dimensionless offset of the gravity center axis measured from the elastic axis; m, m_1 and m_2 are, respectively, the mass of the airfoil, the first and the second supporting devices; J_c is the moment of inertia of the airfoil about the gravity center axis; b is the airfoil semi-chord; c_1 and c_2 are the damping coefficients of the two plunge DOFs, respectively; V_1 and V_2 are the voltage outputs of the two transducers, respectively; θ is the electromechanical coupling factor; C_p is the equivalent capacitance of the transducers; R_1 and R_2 are the load resistances in respective circuits. Note that the structural nonlinearities are not taken into account in this work. α_{eff} is the effective angle of attack, and $\alpha_{\mathrm{eff}}=\alpha+\dot{h}/U-(0.5+a)b\dot{\alpha}/U$, where h is the plunge displacement of the elastic axis, positive downward, and α is the pitch displacement, positive nose up; $L=\rho U^2 bC_l$, $D=\rho U^2 bC_d$ and $M=2\rho U^2 b^2 C_m$ are the aerodynamic lift (normal to the direction of the resultant flow velocity, positive upward), drag (along the resultant flow velocity, positive leeward), and moment (positive nose up) acting at the airfoil one-quarter-chord axis, respectively, where ρ is the air density and U is flow velocity. The aerodynamic coefficients are calculated using the ONERA dynamic stall model [29] to consider the effects of flow separation due to large airfoil amplitudes. The aerodynamic model used in this work is

$$C_z = C_{za} + C_{zb}, \tag{4}$$

$$C_{za} = t_\tau s_{z1}\dot{\alpha}_{\mathrm{eff}} + t_\tau^2 s_{z2}\ddot{\alpha} + t_\tau s_{z3}\dot{\alpha} + c_{z\gamma}, \tag{5}$$

$$t_\tau \dot{C}_{z\gamma} + \lambda_1 C_{z\gamma} = \lambda_1 a_{oz} \;\; \alpha_{\mathrm{eff}} + t_\tau \dot{\alpha} \;\; + \lambda_2 a_{oz} \;\; t_\tau \dot{\alpha}_{\mathrm{eff}} + t_\tau^2 \ddot{\alpha} \;\;, \tag{6}$$

$$t_\tau^2 \ddot{C}_{zb} + t_\tau r_{1z}\dot{C}_{zb} + r_{2z}C_{zb} = -r_{2z}\Delta C_z - t_\tau r_{3z}\dot{\alpha}_{\mathrm{eff}} \; \partial \Delta C_z / \partial \alpha_{\mathrm{eff}} \;, \tag{7}$$

$$C_d = C_{da} + C_{db}, \tag{8}$$

$$t_\tau^2 \ddot{C}_{d2} + t_\tau r_{1d}\dot{C}_{d2} + r_{2d}C_{d2} = -r_{2d}\Delta C_z - t_\tau r_{3d}\dot{\alpha}_{\mathrm{eff}}, \tag{9}$$

where subscript z can be l or m to indicate, respectively, lift or moment coefficient; $t_\tau=b/U$. Subscripts a and b refer to the linear and nonlinear part of the aerodynamics, respectively; the coefficients are $s_{l1}=\pi$, $s_{l2}=\pi/2$, $s_{l3}=0$, $s_{m1}=-\pi/4$, $s_{m2}=-3\pi/16$, $s_{m3}=-\pi/4$, $\lambda_1=0.15$, $\lambda_2=0.55$, $a_{ol}=5.9$, $a_{om}=0$, $c_{d1}=0.014$, $r_{1d}=0.32$; the terms with respect to the nonlinear aerodynamics in Eqs. (7) and (9) are given in the **Appendix A**. The relationship between h_1, h_2 and h, α can be expressed via a transfer matrix

$$\begin{bmatrix} h \\ \alpha \end{bmatrix} = \frac{1}{d}\begin{bmatrix} d-a+d_1 & a-d_1 \\ -1/b & 1/b \end{bmatrix}\begin{bmatrix} h_1 \\ h_2 \end{bmatrix}. \tag{10}$$

To verify the advantage of EH based on the double-plunge airfoil, an equivalent pitch-plunge airfoil-based EH model is built. Shown in Fig. 2, the plunge DOF of the equivalent model is coupled with two transducers in parallel to ensure the use of the same amount of piezoelectric material. For this pitch-plunge airfoil-based harvester, the dynamics are

$$m_T\ddot{h} + mx_\alpha b\ddot{\alpha} + c_h\dot{h} + k_h h - \theta V_1 - \theta V_2 = -\left[L\cos(\alpha_{\text{eff}} - \alpha) + D\sin(\alpha_{\text{eff}} - \alpha)\right], \quad (11)$$

$$mx_\alpha b\ddot{h} + \left[J + m(x_\alpha b)^2\right]\ddot{\alpha} + c_\alpha\dot{\alpha} + k_\alpha\alpha = \frac{2ab+b}{4}\left[L\cos(\alpha_{\text{eff}} - \alpha) + D\sin(\alpha_{\text{eff}} - \alpha)\right] + M, \quad (12)$$

$$C_p\dot{V}_1 + V_1/R_1 + \theta\dot{h} = 0,\ C_p\dot{V}_2 + V_2/R_2 + \theta\dot{h} = 0, \quad (13)$$

where k_h and k_α are, respectively, the stiffness coefficients of the plunge and pitch DOFs; c_h and c_α are the damping coefficients of these two DOFs, respectively; m_{T} is the total mass of the airfoil together with its supporting devices; J is the moment of inertia of the pitch-plunge airfoil about the gravity center axis. The relationships between the mass, stiffness, and damping coefficients of the two harvesters are derived as

$$m_{\text{T}} = m + m_1 + m_2,\ J = J_{\text{c}} + m_1(a - d_1)^2 b^2 + m_2(d - a + d_1)^2 b^2, \quad (14)$$

$$k_h = k_1 + k_2,\ k_\alpha = k_1(a - d_1)^2 b^2 + k_2(d - a + d_1)^2 b^2, \quad (15)$$

$$c_h = c_1 + c_2,\ c_\alpha = c_1(a - d_1)^2 b^2 + c_2(d - a + d_1)^2 b^2. \quad (16)$$

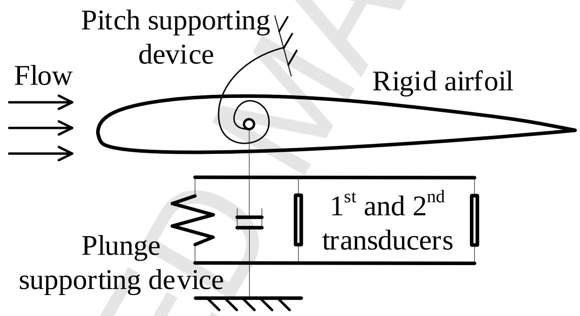

Fig. 2. Schematic of an equivalent pitch-plunge airfoil-based harvester.

For EH based on two transducers via respective circuits, the total harvested energy is evaluated by the average power output

$$\bar{P} = \frac{1}{t_2 - t_1}\left(\int_{t_1}^{t_2}\frac{V_1^2}{R_1}\text{d}t + \int_{t_1}^{t_2}\frac{V_2^2}{R_2}\text{d}t\right), \quad (17)$$

where t_1 to t_2 is a period of time in which the transient response has been dissipated.

Results and Discussions

The dynamic equations are solved numerically using the Runge-Kutta method. For all results presented, the initial conditions are $\dot{h}_1$=0.01 and zeroes for the rest of the state variables. The value of the system parameters are: m=2.049 kg; m_1=m_2=10.338 kg; b=0.135 m; x_α=0.331; d_1=−1; d=1; J_c=0.0517 kg·m^2; c_1=c_2=27.43 kg·s^{-1}; k_1=k_2=1000 N·m^{-1}; θ=1.55×10^{-3} N·V^{-1}; C_p=1.2×10^{-7} F; R_1=R_2=1×10^6 Ω. The air density is 1.225 kg·m^{-3} and the viscosity coefficient is 1.78×10^{-5} Pa·s. To calculate the average power output, the time period t_1 to t_2 in Eq. (17) corresponds to the last 10 s of the total simulation time (30 s) where the transient responses are observed to be completely dissipated. The cut-in speed (flutter speed) of the harvester is determined as 28.4 m·s^{-1}. The time history results as the flow velocity is 30 m·s^{-1} are shown in Fig. 3.It is shown that the plunge amplitude and voltage output of the second plunge DOF is larger than that of the first plunge DOF. Besides, the effective angle of attack can be large enough to cause flow separation, e.g., the amplitude is 22° shown in Fig. 3 (b). This demonstrates the necessity of using the dynamic stall model to calculate the aerodynamics in this work.

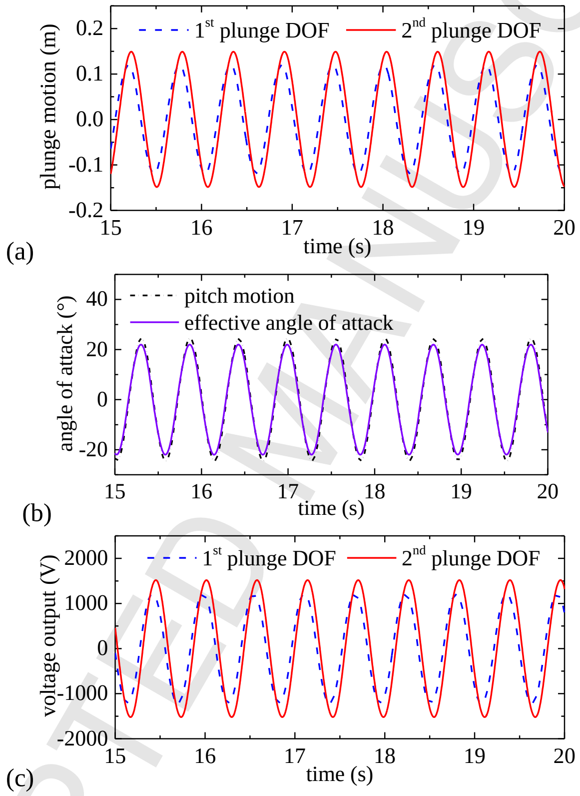

Fig. 3. Time histories of (a) the plunge motion, (b) the pitch motion and (c) the voltage output of the proposed harvester as the flow velocity is 30 m·s^{-1}.

The double-plunge airfoil-based energy harvester is numerically compared with its pitch-plunge counterpart. The cut-in speed of the latter is firstly obtained as 30.2 m·s^{-1}, which is larger than that of the former. This result shows that the use of the double-plunge configuration improves the EH performance with a relative reduction 6% of the cut-in speed. The average power outputs of these two harvesters with the flow velocity are compared in Fig. 4. Obviously, the power output using double-plunge configuration is larger than that using the pitch-plunge configuration. The relative enhancement of the power output is shown in Fig. 4 by a dotted line. It can be seen that the enhancement in percentage varies with the flow velocity and fluctuates between 4%

and 10%. Besides, the relationship between the power outputs of the two harvesters and the flow velocity is approximately piecewise linear. Specifically, the slopes of the two curves increase at 36 m·s^{-1} and then descend as the flow velocity is beyond 37 m·s^{-1}.

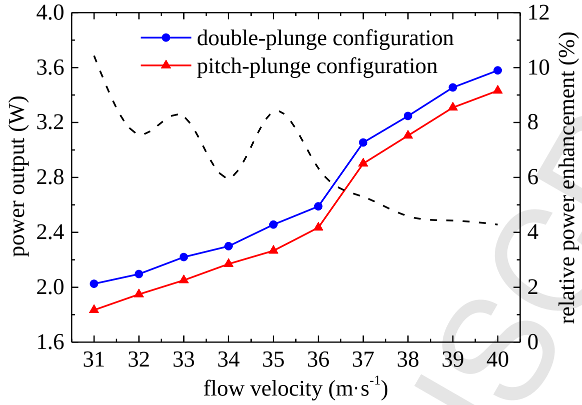

Fig. 4. Average power outputs of the harvesters with double-plunge and pitch-plunge configurations with the flow velocity (solid lines), and the relative enhancement of the power output (dash line).

The comparison of the average power outputs of two plunge DOFs with the flow velocity is shown in Fig. 5. In this work, the first plunge supporting device is at the leading edge of the airfoil while the second one is at the mid-chord axis. Also, the parameters of the two plunge supporting devices are set identically. It can be seen that the power output from the second plunge DOF is larger than that from the first plunge DOF. Specifically, the former is approximately 50% larger than the latter with varying flow velocity.

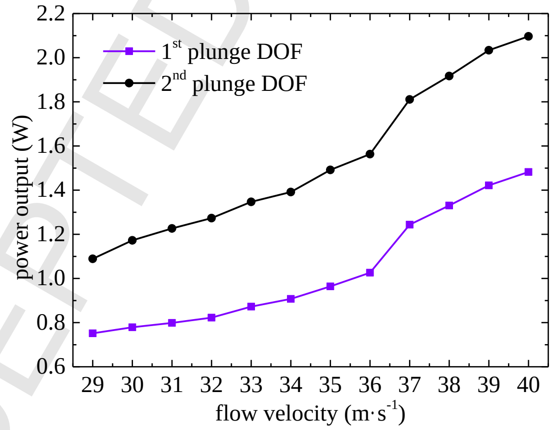

Fig. 5. Average power outputs of the first and second plunge DOFs with the flow velocity.

Conclusion

In summary, this letter proposes a piezoaeroelastic energy harvester based on an airfoil with double plunge DOFs. The dynamic equations of this harvester and an equivalent well-explored pitch-plunge airfoil-based harvester are presented. It is numerically demonstrated that the proposed harvester out performs its counterpart using the pitch-plunge configuration in terms of the average power output and the cut-in speed. Specifically, it is found that the former generates 4% to 10% more power with varying flow velocities while reducing 6% of the cut-in speed than the latter. It is also shown that the second downstream plunge supporting device of the proposed harvester has larger plunge amplitude and hence yields 50% more power output compared with the first upstream one.

Appendix A

The terms with respect to the nonlinear aerodynamics in Eqs. (7) and (9) are:

$$r_{1z} = 0.25 + 0.1\Delta C_l^2,\ r_{2z} = \left(0.2 + 0.1\Delta C_l^2\right)^2,\ r_{3z} = -0.6\Delta C_l^2\left(0.2 + 0.1\Delta C_l^2\right)^2, \quad \text{(A.1)}$$

if the Reynolds number is larger than 3.4×10^5, and

$$r_{1z} = 0.25 + 0.4\Delta C_l^2,\ r_{2z} = \left(0.2 + 0.23\Delta C_l^2\right)^2,\ r_{3z} = -2.7\Delta C_l^2\left(0.2 + 0.23\Delta C_l^2\right)^2, \quad \text{(A.2)}$$

if the Reynolds number is smaller than 3.4×10^5. Besides,

$$\Delta C_l = \begin{cases} 6.3\left(\alpha_{\text{eff}} - \alpha_1\right) - 0.4\left(\alpha_{\text{eff}} - \alpha_2\right), \alpha_{\text{eff}} > \alpha_2, \\ 6.3\left(\alpha_{\text{eff}} - \alpha_1\right), \alpha_1 < \alpha_{\text{eff}} \le \alpha_2, \\ 0, -\alpha_1 < \alpha_{\text{eff}} \le \alpha_1, \end{cases} \quad \text{(A.3)}$$

$$\Delta C_m = \begin{cases} 0.65\left(\alpha_{\text{eff}} - \alpha_1\right) - 0.48\left(\alpha_{\text{eff}} - \alpha_2\right), \alpha_{\text{eff}} > \alpha_2, \\ 0.65\left(\alpha_{\text{eff}} - \alpha_1\right), \alpha_1 < \alpha_{\text{eff}} \le \alpha_2, \\ 0, -\alpha_1 < \alpha_{\text{eff}} \le \alpha_1, \end{cases} \quad \text{(A.4)}$$

where α_1=0.1396 and α_2=0.3142. In addition,

$$\begin{aligned} &r_{2d} = \left(0.2 + 0.1\Delta C_l\right)^2,\ r_{3d} = \left(0.2 + 0.1\Delta C_l\right)^2\left(-0.015\Delta C_l^2\right), \\ &\Delta C_d = -0.042\alpha_{\text{eff}} - 0.1473\alpha_{\text{eff}}^2 - 4.923\alpha_{\text{eff}}^3. \end{aligned} \quad \text{(A.5)}$$

Acknowledgements

This work was supported by the National Natural Science Foundation of China (No. 11402014, 11572023); and the Royal Academy of Engineering for the project "Fast Nonlinear Aeroelastic Search for Loads Assessment" (No. NCRP/1415/51).

References

[1] A. Abdelkefi, Aeroelastic energy harvesting: a review, Int. J. Eng. Sci. 100 (2016) 112-135.

[2] A. Truitt, S.N. Mahmoodi, A review on active wind energy harvesting designs,

Int. J. Precis. Eng. Man. 14 (2013) 1667-1675.

[3] M. Piñeirua, O. Doaré, S. Michelin, Influence and optimization of the electrodes position in a piezoelectric energy harvesting flag, J. Sound Vib. 346 (2015) 200-215.

[4] J.A. Dunnmon, S.C. Stanton, B.P. Mann, et al., Power extraction from aeroelastic limit cycle oscillations, J. Fluid Struct. 27 (2011) 1182-1198.

[5] A. Bibo, M.F. Daqaq, On the optimal performance and universal design curves of galloping energy harvesters, Appl. Phys. Lett. 104 (2014) 23901.

[6] Y. Yang, L. Zhao, L. Tang, Comparative study of tip cross-sections for efficient galloping energy harvesting, Appl. Phys. Lett. 102 (2013) 64105.

[7] A. Abdelkefi, J.M. Scanlon, E. Mcdowell, et al., Performance enhancement of piezoelectric energy harvesters from wake galloping, Appl. Phys. Lett. 103 (2013) 33903.

[8] H. Jung, L. Seung-Woo, The experimental validation of a new energy harvesting system based on the wake galloping phenomenon, Smart Mater. Struct. 20 (2011) 55022.

[9] L. Ding, L. Zhang, M.M. Bernitsas, et al., Numerical simulation and experimental validation for energy harvesting of single-cylinder VIVACE converter with passive turbulence control, Renew. Energ. 85 (2016) 1246-1259.

[10] J. Xu-Xu, A. Barrero-Gil, A. Velazquez, A theoretical study of the coupling between a vortex-induced vibration cylindrical resonator and an electromagnetic energy harvester, Smart Mater. Struct. 24 (2015) 115009.

[11] J.A.C. Dias, C. De Marqui Jr, A. Erturk, Hybrid piezoelectric-inductive flow energy harvesting and dimensionless electroaeroelastic analysis for scaling, Appl. Phys. Lett. 102 (2013) 44101.

[12] C. De Marqui Jr, A. Erturk, Electroaeroelastic analysis of airfoil-based wind energy harvesting using piezoelectric transduction and electromagnetic induction, J. Intel. Mat. Syst. Str. 24 (2013) 846-854.

[13] M. Bryant, E. Garcia, Modeling and testing of a novel aeroelastic flutter energy harvester, J. Vib. Acoust. 133 (2011) 11010.

[14] A. Erturk, W.G.R. Vieira, C. De Marqui Jr, et al., On the energy harvesting potential of piezoaeroelastic systems, Appl. Phys. Lett. 96 (2010) 184103.

[15] V.C. Sousa, M. de M Anicézio, C. De Marqui Jr, et al., Enhanced aeroelastic energy harvesting by exploiting combined nonlinearities: theory and experiment, Smart Mater. Struct. 20 (2011) 94007.

[16] J. Bae, D.J. Inman, Aeroelastic characteristics of linear and nonlinear piezo-aeroelastic energy harvester, J. Intel. Mat. Syst. Str. 4 (2014) 401-416.

[17] A. Abdelkefi, M.R. Hajj, Performance enhancement of wing-based piezoaeroelastic energy harvesting through freeplay nonlinearity, Theor. Appl. Mech. Lett. 3 (2013) 41001.

[18] V.C. Sousa, C. De Marqui Jr, Airfoil-based piezoelectric energy harvesting by exploiting the pseudoelastic hysteresis of shape memory alloy springs, Smart Mater. Struct. 24 (2015) 125014.

[19] M. Bryant, E. Wolff, E. Garcia, Aeroelastic flutter energy harvester design: the sensitivity of the driving instability to system parameters, Smart Mater. Struct. 20 (2011) 125017.

[20] A. Abdelkefi, A.H. Nayfeh, M.R. Hajj, Enhancement of power harvesting from piezoaeroelastic systems, Nonlinear Dynam. 68 (2012) 531-541.

[21] A. Abdelkefi, A.H. Nayfeh, M.R. Hajj, Modeling and analysis of piezoaeroelastic energy harvesters, Nonlinear Dynam. 67 (2012) 925-939.

[22] A. Abdelkefi, M. Ghommem, A.O. Nuhait, et al., Nonlinear analysis and enhancement of wing-based piezoaeroelastic energy harvesters, J. Sound Vib. 333 (2014) 166-177.

[23] A. Abdelkefi, A.H. Nayfeh, M.R. Hajj, Design of piezoaeroelastic energy harvesters, Nonlinear Dynam. 68 (2012) 519-530.

[24] A. Bibo, M.F. Daqaq, Investigation of concurrent energy harvesting from ambient vibrations and wind using a single piezoelectric generator, Appl. Phys. Lett. 102 (2013) 243904.

[25] A. Bibo, M.F. Daqaq, Energy harvesting under combined aerodynamic and base excitations, J. Sound Vib. 332 (2013) 5086-5102.

[26] A. Abdelkefi, A.O. Nuhait, Modeling and performance analysis of cambered wing-based piezoaeroelastic energy harvesters, Smart Mater. Struct. 22 (2013) 95029.

[27] J.A.C. Dias, C. De Marqui Jr, A. Erturk, Three-degree-of-freedom hybrid piezoelectric-inductive aeroelastic energy harvester exploiting a control surface, AIAA J. 53 (2014) 394-404.

[28] J. Bae, D.J. Inman, A preliminary study on piezo-aeroelastic energy harvesting using a nonlinear trailing-edge flap, Int. J. Aeronaut. Space Sci. 16 (2015) 407-417.

[29] P. Dunn, D. John, Nonlinear stall flutter and divergence analysis of cantilevered

graphite/epoxy wings, AIAA J. 30 (1992) 153-162.

Highlights

- A double-plunge airfoil-based piezoaeroelastic energy harvester is proposed.
- The dynamic model of the proposed harvester is presented.
- The proposed harvester generates higher power output than conventional designs.
- The proposed harvester has lower cut-in speed than conventional designs.